Bulletin of Environment, Pharmacology and Life Sciences
Bull. Env.Pharmacol. Life Sci., Vol 4 [Spl issue 1] 2015: 01-10

Online ISSN 2277-1808
Journal's URL:http://www.bepls.com
CODEN: BEPLAD
Global Impact Factor 0.533
Universal Impact Factor 0.9804

FULL LENGTH ARTICLE **OPEN ACCESS**

Numerical Examination of the Effect Of The Location Of Flowmeters In Intakes On Flow-Velocity Measurement Accuracy

Sohrab karimi[1], Hossein Bonakdari [2,4*], Azadeh Gholami[3]
[1]M.Sc. Student, Department of Civil Engineering, Razi University, Kermanshah, Iran
[2]Associate Professor, Department of Civil Engineering, Razi University, Kermanshah, Iran
[3]Ph.D. Student, Department of Civil Engineering, Razi University, Kermanshah, Iran
[4]Water and Wastewater Research Center, Razi University, Kermanshah, Iran
[*]Corresponding author, e-mail: bonakdari@yahoo.com

ABSTRACT
Intakes are used to control water and to deviate a part of the flow in agricultural networks and water transfer systems. The flow velocity is measured by flowmeters in order to calculate the discharge passing through the channels. The three-dimensional and complex nature of the flow in the intakes and the presence of strong secondary flows in the cross section cause a difference between the velocity measured by the flowmeter and the flow velocity in the channel. The manner in which the flowmeter is located in the intake, the velocity of the passing flows, and etc. affect the difference between the flowmeter and the actual mean flow velocity. The objectives of this study include examining the following issues in different width ratios: (a) simulating the model of the intake flow through the ANSYS- CFX software (b) examining the effect of flow deviation in intakes on flow hydraulics and velocity distribution (c) examining the effect of the location of the flowmeter on the velocity measurement accuracy in the intake channel. The results obtained in different width ratios indicate that the measurement accuracy decreases in the flow separation zone and flow compression zone when the velocity is measured by a flowmeter and a numerical model due to the velocity fluctuations and flow hydraulics complexity. Therefore the flowmeters must be installed in the middle areas and the sides of the channel in order to increase the measurement accuracy so that the results will be more consistent with the actual velocity of the channel.
***Key terms**: intakes, flow deviation, flow velocity, location of the flowmeter, ANSYS-CFX.*

INTRODUCTION

Intakes are amongst hydraulic structures which are used for the purposes of controlling and deviating flow in agricultural and irrigation networks, sewer systems. Determining the model of the flow which is entering the branch channels from the main channel is of utmost important in these hydraulic structures. A part of the flow in the main channel is deviated and enters the branch channel when impounding the river due to the suction force applied to it, as a result, flow separation zone and flow compression zone are formed near the mouth of the intake channel. The flow deviated into the intake has complex properties. The flow particles rotate in the separation zone near the entrance wall of the intake channel and the longitudinal velocity of the flow has decreased and it will increase in the opposite direction of the flow. The longitudinal velocities intensely increase in the compression zone due to the density of the flow lines and it reaches its maximum levels therefore measuring the flow velocity in the flow separation zone and the flow compression zone is difficult and accompanied with error [1-7].

They install flowmeters in intakes in order to compute the flow discharge and measure the flow velocity. Flowmeters rely on measuring the velocity and calculate the discharge using the continuity equation as the multiplication of the mean velocity by the wet cross section ($Q = A(h) \times U_{mean}$). The A(h) cross section is calculated through measuring the height of the free surface (h) and using precise geometrical information. Determining the mean velocity passing through the cross section requires special knowledge [12]. Velocity sensors present data holding the assumption that the data represents the entire cross section it must be noted that the measured velocity is often different from the mean velocity of the cross section [13]. The relationship between the measured value and the actual mean velocity of the flow depends on the volume of the sample of the velocity sensor and the hydrodynamic specifications of the measurement location [14, 15]. The area of the space being examined by the flowmeter is a three-dimensional volume and the flowmeters sample a limited volume of the flow [16]. The mean velocity is

calculated and assumed based on this calculated volume and this velocity is equal to the mean velocity in the entire section [17].

Ramamurthy et al. [3], used the limited volume method and took measures in three dimensionally modeling a 90- degree intake with a rectangular cross section. These authors compared the numerical results with the experimental results and came to the conclusion that the utilized limited volume model has a suitable accuracy. Also they examined the velocity within the intakes and concluded that the vortex strength ratio has a direct relationship with the discharge ratio. Mignot et al., [8] conducted their numerical studies on the measurement error of the flowmeters in diversion channels. They calculated the changes of the created error through changing the location of the flowmeters in the channel and came to the conclusion that the values read by the flowmeters may be different from the actual mean velocity in the channel by more than 60%.

We will examine the effect of the location of the flowmeter in intake channel on the flow velocity measurement accuracy in this study. There are no available experimental results in some flow conditions in this examination therefore it is necessary to define and verify a numerical model. In order to do that, Ramamurthy et al. (2007) [3] experimental model has been three- dimensionally simulated by the ANSYS-CFXX software in different w_r width rations. The longitudinal velocities in the experimental model have been compared with the velocities obtained from the CFX model in order to verify the CFX model, following that, we will evaluate the accuracy of flowmeters in three different locations in the intake channel through the results obtained from the CFX model. In the first location, he flowmeter reads the longitudinal velocities located in the vertical column in the middle of the channel and in the second location the flowmeter measures the longitudinal velocities located in two vertical columns these columns are located in equal distances in the cross section of the branch channel and in the third location, the flowmeter measures the velocities in three vertical columns and like the second location, these columns are located in equal transverse distances in the branch channel and then the flowmeter measurement accuracy will be calculated in each of the locations from the first location to the third location and they will be compared to one another.

THE EXPERIMENTAL MODEL

Ramamurthy et al. (2007) conducted their experiments in a horizontal channel with a 90- degree Diversion which directs the flow in the main and the branch channel (Figure 1). The length of the main channel is equal to 6.198 meters and its branch is 2.794 meters long. The widths of the channels are equal to 0.61 meters and their heights are equal to 0.305 meters. The branch channel is located 2.794 meters away from the beginning of the main channel (Figure 1).

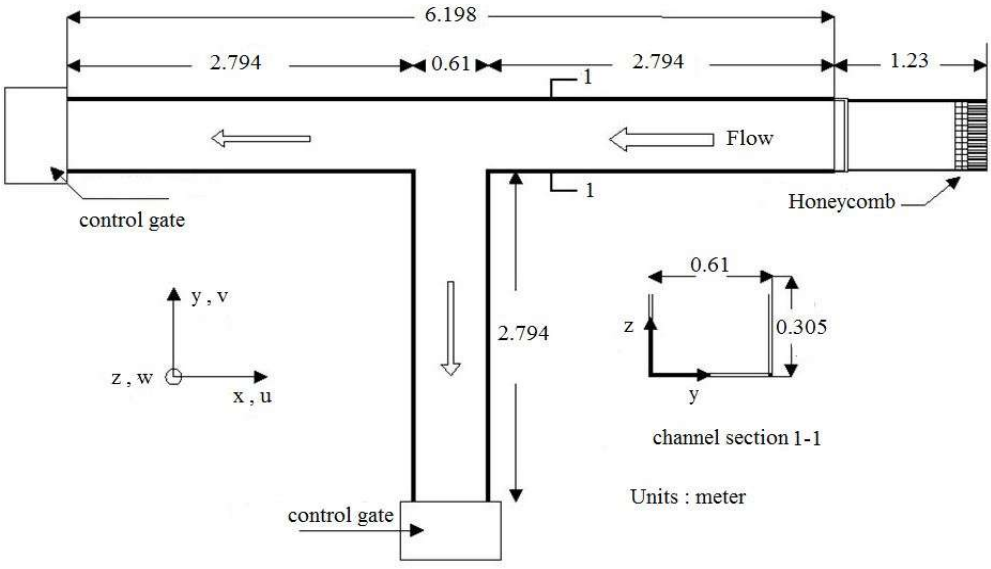

Figure 1. the plan of the experimental channel used in this study (Ramamurthy et al., 2007 [3])

Taking into account that w^*_m is the width of the main channel and w^*_b is the width of the branch channel the channel used by Ramamurthy et al., (2007) has a width ratio of 1 ($w_r = w^*_b / w^*_m = 1$) the discharge entering the entrance of the main channel is equal to $Q_u = 0.046\ m^3/s$ and it is equal to $Q_b = 0.038\ m^3/s$ in the branch channel. The ratio of the branch channel discharge to the main channel discharge ($Q_r = Q_b / Q_u$) is equal to 0.838. All the parameters have been made dimensionless by the channel width ($B = 0.61\ ^m$) and

the main channel upstream critical velocity (v_c) in the experiments conducted by Ramamurthy et al. (2007) and so the coordinate axes are defined in a dimensionless manner ($x^*=x/b$ ،$y^*=y/b$, and $z^*=z/b$). The dimensionless velocities in x, y, and z coordinates are marked as u*, v*, and w* respectively. The measurement locations in the channels can be seen in Figure 2.

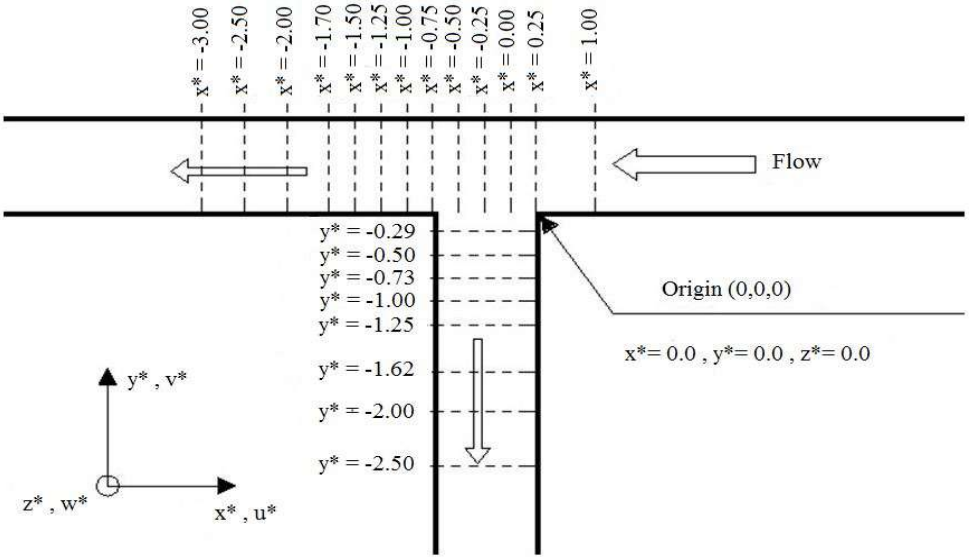

Figure 2. the measurement locations in the channels (Ramamurthy et al., 2007)[3]

The numerical model

As the speed and the capacity of computers increased in the recent decades the application of numerical computation of fluid flows, which is called computational fluid dynamics (CFD), are increasing in engineering sciences. One of the codes of the computational fluid dynamics is ANSYS- CFX which uses the finite volume method to solve complete incompressible Reynolds- averaged Navier- Stokes equations. Most flows often occur in high Reynolds the experimental results indicated that the Reynolds number Re is between 15,000 and 30,000 in junction flow. We will therefore need to define an appropriate turbulence model in order to reach accurate numerical answers. The two main equations for fluid movement in open channel intake are:

Continuity equation for incompressible fluids:

$$\frac{\partial \rho}{\partial t}+\frac{\partial \rho U}{\partial x}+\frac{\partial \rho V}{\partial y}+\frac{\partial \rho W}{\partial z}=0 \rightarrow \frac{\partial \rho}{\partial t}+\mathrm{div}(\rho U)=0 \qquad (1)$$

The three Reynolds time- averaged Navier- Stokes momentum equation for steady condition and an incompressible turbulent fluid:

$$\frac{\partial}{\partial x}\left(\rho u_j\right)+\frac{\partial}{\partial x_j}\left(\rho u_i u_j\right)= \quad \frac{\partial P}{\partial x_i}+\frac{\partial}{\partial x_j} \quad \mu \quad \frac{\partial u_i}{\partial x_j}+\frac{\partial u_j}{\partial x_i} \quad \frac{2}{3}\delta_{ij}\frac{\partial u_i}{\partial x_j} \quad +\frac{\partial}{\partial x_i}\left(\quad \rho\overline{u_i' u_j'}\right) \qquad (2)$$

$\rho\overline{U'iU'j}$ is also Reynolds stress tensor and we will need to introduce a turbulence model to determine it. k-ω turbulence model of Wilcox, [10] has been used in this study and two transport equations are solved in it one for the turbulent kinetic energy ,k (Eq.3), and the other one for the turbulent frequency ,ω (Eq.4)[10, 11]:

$$\frac{\partial(\rho k)}{\partial t}+\frac{\partial}{\partial x_j}\left(\rho u_j k\right)=\frac{\partial}{\partial x_j} \quad \mu+\frac{\mu_t}{\sigma_k} \quad \frac{\partial k}{\partial x_j} \quad +p_k\beta'_{-} \quad \rho k\omega \qquad (3)$$

$$\frac{\partial(\rho\omega)}{\partial t}+\frac{\partial}{\partial x_j}\left(\rho u_j \omega\right)=\frac{\partial}{\partial x_j} \quad \mu+\frac{\mu_t}{\sigma_\omega} \quad \frac{\partial \omega}{\partial x_h} \quad +\alpha\frac{\omega}{k}p_k \_ \beta\rho\omega^2 \qquad (4)$$

Where p_k is the production rate of turbulence, for incompressible flow given by:

$$p_k=\mu_t \quad \frac{\partial u_i}{\partial x_j}+\frac{\partial u_j}{\partial x_i} \quad \frac{\partial u_i}{\partial x_j} \qquad (5)$$

The model five constant assume their standard values: $\beta'=0.09$, $\alpha=5.9$, $\beta=0.075$, $\sigma_k=2$, $\sigma_\omega=2$.
Since the momentum equation is elliptic, boundary conditions must be introduced. The depth h is considered in the entrance boundary of the flow mean velocity U= Q/A and the constant depth h and zero relative average statistic pressure have been considered in the output boundary according the experimental model. The wall boundaries have been considered in accordance to the flume of the smooth with no slip condition experimental model. The velocity indexes have been considered zero in the areas near the wall in accordance with the standard wall function method. Normal speed has been used in order to define the boundary conditions in the numerical model for the purposes of simulating Ramamurthy et al.'s (2007) experimental model, the entrance of the main channel, and the exit of the intake and the main channel. The "fixed wall" and "smooth wall" conditions have been used for the walls and the floor of the channel and the "opening" boundary condition has been used for the upper surface of the channel. The definition of the free surface has been specified according to Eulerian viewpoint and the volume of fluid (VOF) has been used to define the flow's free surface.
Proper gridding results in an increase in the speed of executing the model regarding the numerical models. Therefore we have divided the main channel into three separate sections in the simulated model presented in this study in order to optimally execute the gridding. The length of its first section is located in the main channel upstream and it is 2.794 meters, the length of its second section is 0.61 meters and it is located in the middle of the main channel and the length of its third section is equal to 2.794 meters and located in the main channel downstream. The size of the cells in the main channel upstream and downstream is 1×0.5×0.5 centimeters in the main channel upstream and downstream and the size of the cells in the middle section is 0.5×0.5×0.5. The sizes of the cells of the intake channel network have been selected to be 0.5×0.5×0.5. Figure 3 shows the plan and view of the gridding of the computational field in the 90- degree intake.

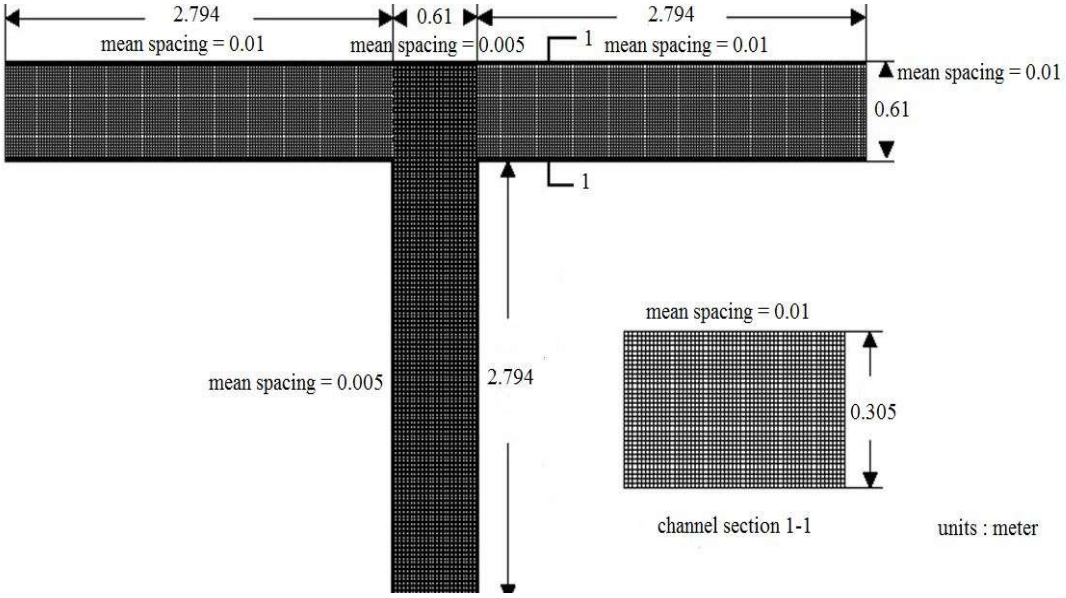

Figure 3. gridding of the plan and the cross section of the model simulated through the use of ANSYS- CFX

The results of the numerical model

The experimental model presented by Ramamurthy et al., [3] will first be simulated in this section through the use of ANSYS- CFX and then the results of the numerical model are compared to the results of the experimental model and the simulation accuracy will be examined. And then, taking into consideration the fact that Ramamurthy et al., (2007) conducted limited experiments and the ability of the numerical model in simulating the flow field, a number of models will be presented for different width ratios through using the numerical model and its results will be used in presenting an equation to predict the mean velocity. Following that an equation will be presented by using the GEP to predict the initial velocity.

Verifying the results of the CFX model

The results of Ramamurthy et al.'s (2007)[3] experimental model have been used in this section to examine the accuracy of the results of the numerical model. The longitudinal dimensionless velocities (V*) obtained from the CFX model are compared with the experimental results in Figure 4. The horizontal axis

in this figure shows the transverse distances (x*) in the branch channel and the vertical axis indicates the flow depth z*. the results of the numerical model and the experimental model have been compared in the discharge ration (Q_r= Q_b/ Q_u) of 0.838 and the results of the verification have been evaluated in three cross sections of y*= -1.62, -1.00, -0.29 of the branch channel with regard to the cross sections measured in the experimental model.

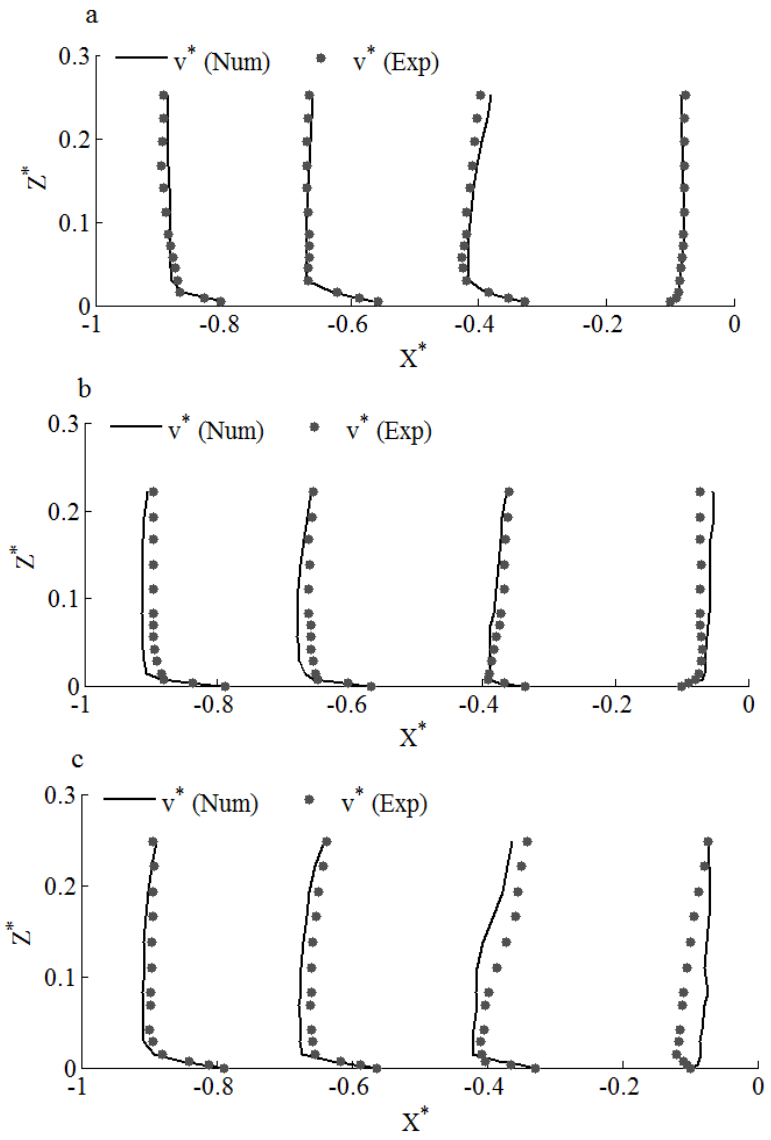

Fig 4. Verification graphs between the results of the CFX model and the Ramamurthy et al.'s (2007) experimental model in: a) y*=-0.29, b) y*=-1.00 and c) y*=-1.62

The two statistical indexes Root Mean Square Error (RMSE) and Mean Absolute Percentage Error (MAPE) are used to examine the preciseness of the simulation. They are calculated as follows:

$$MAPE = \frac{100}{n} \sum_{i=1}^{n} \frac{\left| V_{EXP_i} \quad V_{CFX_i} \right|}{V_{EXP_i}} \tag{6}$$

$$RMSE = \sqrt{\frac{1}{n} \sum_{i=1}^{n} \left(V_{EXP_i} \quad V_{CFX_i} \right)^2} \tag{7}$$

Where V_{EXP_i} denotes the experimental velocity and V_{CFX} denotes the velocity results of CFX model, respectively.

The MAPE index indicates the difference between experimental and CFX model in form of percentage of actual values and the RMSE index considers weight of larger errors by powering the difference between experimental and CFX model values.

Table 1 shows the results of the numerical model and the experimental model in different cross section (y*) through using statistics indexes. The mean relative error MAPE has been obtained to be 5% in this comparison therefore figure 4 shows a good consistency existing between the results of the CFX model and the results of the experimental model. In three cross section y*= -1.62, -1.0, -0.29, the mean relative error MAPE has been obtained to be approximately 2%, 5.2%, and 6.95% respectively with regard to table 1. The value of RMSE is equal to 0.012, 0.01, and 0.017 for cross section y*= -1.62, -1.0, and -0.29 respectively in the table. In y*= -1.0 and y*= -1.62 in the branch channel downstream, the values of the longitudinal velocity increase in the direction against the flow and the velocities become negative due to the presence of the recirculation zone in the separation zone. In depths of z*= 0.0 to z*= 0.2 and in the contraction zone the velocities are maximum V_{max} and the contraction zone is denser than the flow surface in this area since the flow lines are denser.

Table 1. comparing the results of the numerical model with the results of the experimental model presented by Ramamurthy et al. (2007) by using statistical indexes

	y*= -0.29	y*= -1.00	y*= -1.62
RMSE	0.01	0.012	0.017
MAPE (%)	2.0	5.2	6.95

Examining the flow hydraulic and velocity distribution in different width ratios

When the flow is deviated towards the branch channel from the main channel in intakes, the flow undergoes transverse acceleration due to the effect of the suction force. The flow lines entering the intake channel have a curvy form when affected by this acceleration. The curviness of the flow lines destroys the balance between the lateral pressure gradient, the centripetal force, and the shear stress which creates a secondary flow at the beginning of the intake channel. Also the deviation of the flow from the main channel towards the branch channel creates a separation zone on the side of the branch channel wall. The velocities increase in the depth and reach their maximum level V_{max} in the flow compression zone. Therefore the flow hydraulic is complex in these areas and measuring the velocity here requires great concentration. Numerous factors such as the Froude number, the flow discharge coefficient, and the ratio of the branch channel width to the main channel width affect the separation zone [15- 21].

This section is dedicated to examining the flow hydraulic and the longitudinal velocity profiles in the intake channel. In order to do that the longitudinal velocity v^* contours have been obtained in y*= -1.00 cross section by the CFX model for 0.6, 0.8, 1.00, 1.2, and 1.4 width ratios (Figure 5). The x horizontal axis represents the dimensionless transverse distance in the branch channel and in y*= -1.00 cross section and the z* vertical axis indicates the flow depth which has been made dimensionless. With regard to the figure, as w_r increases from 0.6 to 1.4 the flow lines become denser and the flow compression develops and as we move from x*= 0.0 towards x*= -1.0, the v* longitudinal velocity increases from 0 to 0.4. The negative sign of the v* longitudinal velocity in the figure is because the positive direction of the y* axis has been defined as the opposite direction of the flow. As w_r increases from 0.6 to 1.4 the width of the branch channel increases and the space widens up for the fluid movement in the branch channel and this causes the width of the separation zone and the degree of the compression zone contraction to increase. Therefore w_r= 1.4 is considered as the critical width ratio among the presented width ratios since the separation zone and the compression zone have been completely expanded in this width ratio.

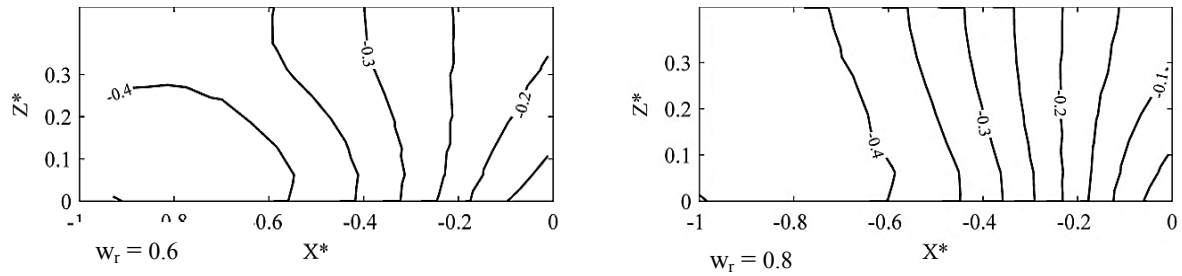

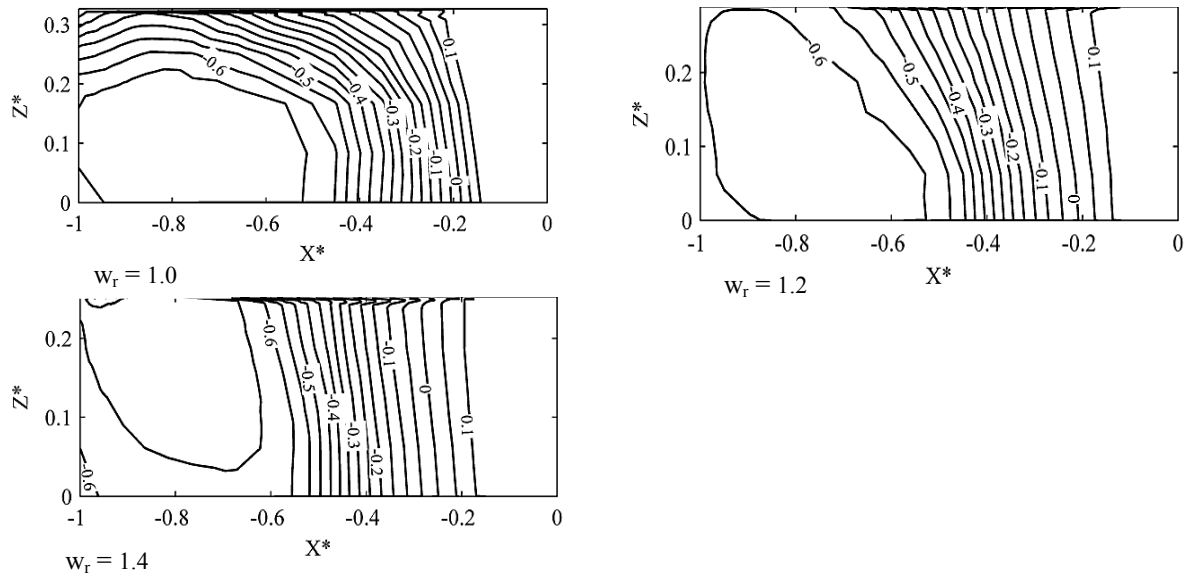

Figure 5. velocity profiles in the branch channel for different width ratios

The effect of the location of the flowmeters on the longitudinal velocities measurement accuracy

One of the most popular methods of determining the flow discharge in intake channels is to measure the flow velocity by a flowmeter. It should be noted that the flow velocity measured by a flowmeter is often different from the mean velocity of the cross section [13]. The relationship between the measured value and the actual mean velocity of the flow depends on the sample volume of the velocity sensor and the hydrodynamic properties of the measurement location [14, 15]. The area of the space examined by the flowmeter is a three- dimensional volume and the flowmeters sample a limited volume of the flow [16]. The mean velocity is calculated and assumed based on this volume this velocity is equal to the mean velocity of the entire cross section [17]. One of the most important factors in selecting a flowmeter is its measurement accuracy. With regard to the error caused by the performance of the flowmeter, the location of the flowmeter in the channel, and … the results obtained from the measurement of the flowmeter are commonly different from the actual results and they are called "measurement error". This section examines the effect of the location of the flowmeter on the longitudinal velocity v* measurement accuracy in intake channel. Considering the verification results and the relatively proper accuracy of the numerical model, the longitudinal velocity v* obtained from the CFX model is considered as the longitudinal velocities v* measured by the flowmeter. These calculations have been done in three different locations for the flowmeters and the constant flow discharge is Q_r= 0.838 in all the locations (Figure 6).

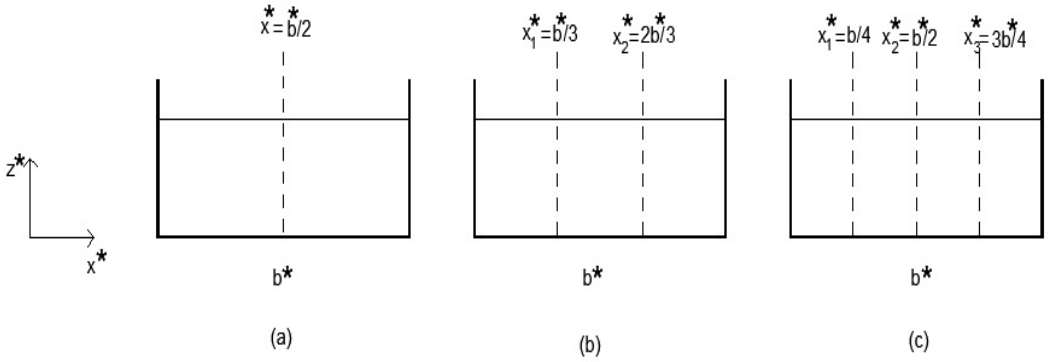

Figure 6. the mean velocity measurement locations by the flowmeter and the numerical model in the branch channel

In accordance to the figure, the v* longitudinal velocities located in the middle column of the intake channel x*= b*/2 have been calculated in different heights in location (a), the channel cross section has been divided into three equal distances in location (b) and the v* longitudinal velocities located in x*= b*/3 and x*= b*/2 distances have been calculated in different heights and the channel cross section has been also divided into 4 equal distance in location (c) and the v* longitudinal velocities which are located

in x*= b*/4, x*= b*/2, and x*= 3b*/4 have been calculated in different heights. The measured longitudinal velocities have been compared with the actual mean velocity of the channel in each of the locations a, b, and c (Figure 7). The horizontal axis in the figure represents the v* longitudinal velocity and the vertical axis indicates the y* specific longitudinal distances in the intake channel. Comparing the measured v* longitudinal velocities in locations a, b, and c will bring us to the conclusion that the measured v* longitudinal velocities are mostly higher than the v_{mean} in w_r= 1.2, 1, 0.8, 0.6 and in location (a) where the flowmeter is located in the middle of the intake channel. According to the figure, the values of the measured v* longitudinal velocities in (b and c) locations are lower than the v_{mean} in some points and they are higher than the v_{mean} in other points. As opposed to the measured v* longitudinal velocities in location (a), the measured v* longitudinal velocities in b and c locations are closer to the v_{mean} and between b and c locations, the results of the c state are closer to the actual value of the v_{mean} since the v* longitudinal velocities are measured in different heights in almost most of the flow areas x*= b*/4, x*= b*/2, and x*= 3b*/4 but only the middle area of the channel x*= b*/2 is measured in location (a) and only the two sides of the channel x*= b*/3 and x*=2b*/3 are measured in location (b). It could be therefore concluded that the larger the number of the v* longitudinal velocity measurement areas in the channel, the more the results obtained are closer to the v_{mean} and the more precise the measurement accuracy. In locations a, b, and c and in w_r= 1.4, 1.2, 1, 0.8, 0.6 there is a difference between the measured v* longitudinal velocities and the v_{mean} in the upstream areas due to the complexity of the flow and the presence of the separation zone and the compression zone but when we move towards the intake downstream the flow becomes less turbulent and since the flow becomes stable this difference decreases and the velocities obtained in the three locations of a, b, and c become closer to the actual v_{mean} of the intake channel.

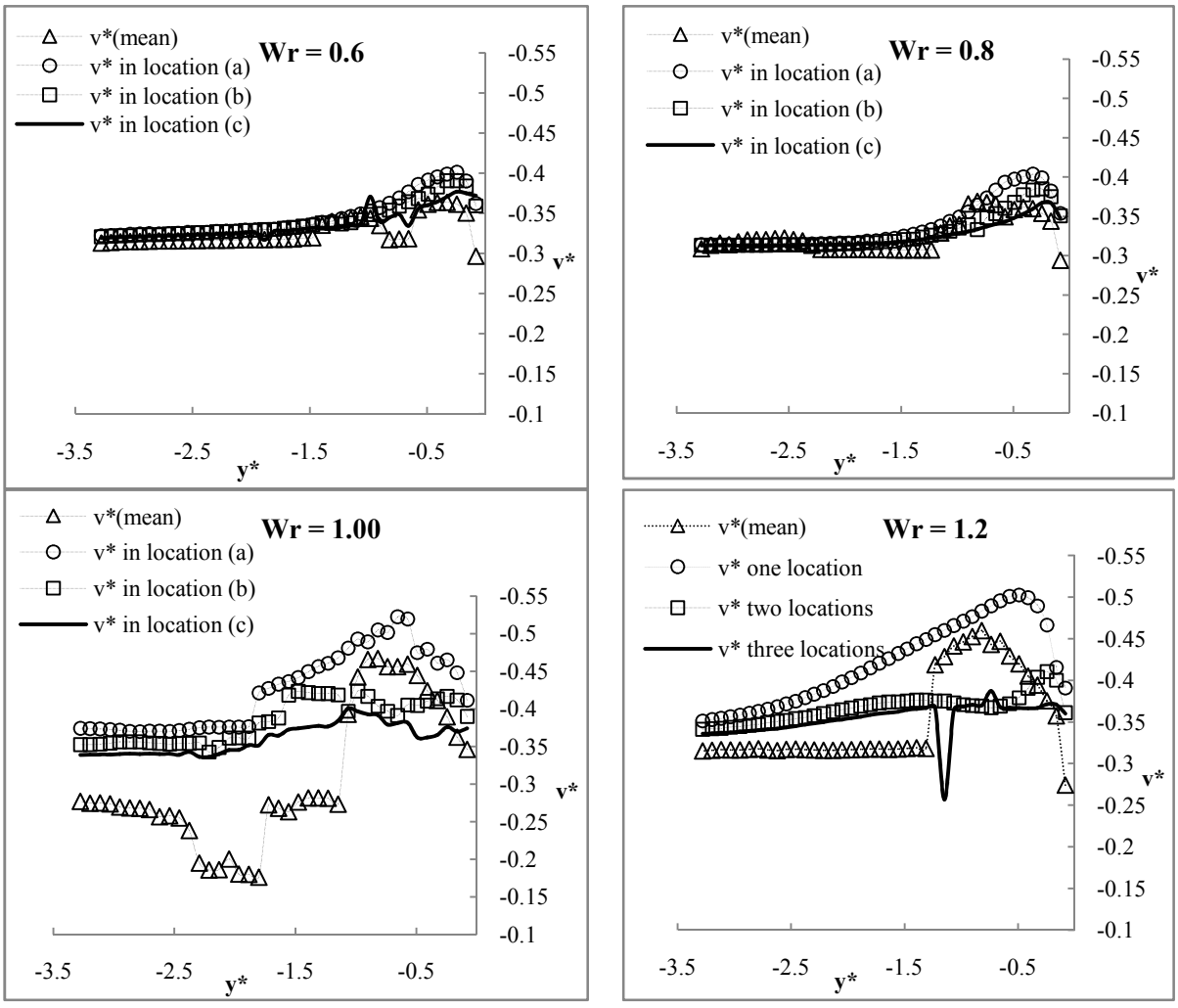

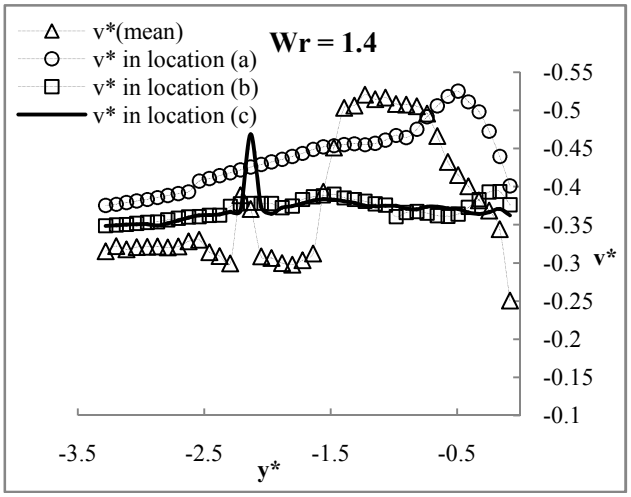

Figure 7. comparing the v* longitudinal velocities measured in locations a, b, and c and the actual v_{mean} in the branch channel

Table 2 uses the statistical indexes and presents the results of the numerical model quantitatively in w_r= 1.4, 1.2, 1. 0.8, 0.6 for location a, b, and c with regard to the results presented on predicting the flow velocity using the CFX model and the flowmeter. The index stated for the purposes of examining the accuracy of the numerical model is the MAPE index. This index shows the difference between the results of the numerical model and the actual values as a percentage of the actual values.

Table 2. the MAPE statistical index obtained for different width ratios

	MAPE %		
LOCATION	(a)	(b)	(c)
w_r = 0.6	5.56	4.61	3.47
w_r = 0.8	4.6	3.65	3.38
w_r = 1.0	47.63	39.31	34.45
w_r = 1.2	20.08	13.40	12.27
w_r = 1.4	22.8	18.45	17.1

It could be seen with regard to the table that in the best state among a, b, and c locations, the value of the presented MAPE is related to location (c) where it is equal to 3.38, 3.47, 34.45, 12.27, and 17.1 in w_r= 1.4, 1.2, 1, 0.8, 0.6 respectively and the worst state is related to location (a) where the MAPE is equal to 4.6, 5.56, 47.63, 20.08, and 22.8 in w_r= 1.4, 1.2, 1, 0.8, 0.6 respectively. According to the table the least value of MAPE is for w_r= 0.6 and in location (C) which has been predicted to be approximately 3.38% and the highest MAPE value is obtained for w_r= 1.4 in location (a) which is approximately 47.63%. These results demonstrate that it is better for the flowmeter to be located in accordance with location (c) and in x*= b*/4, x*= b*/2, and x*= 3b*/ 4 and also for the flow velocity to be measured in these locations as well in order to measure the flow velocity in the intake in all W_r since the velocities are measured in more areas of the intake and will be closer to the actual v_{mean} in the channel. it could be seen from the results that the MAPE values for a, b, and c locations enjoy an ascending trend from w_r= 0.6 to w_r= 1 but it has a descending trend from w_r=1 to w_r= 1.4 this is because from w_r= 0.6 to w_r= 1 the separation zone and the compression zone develop and the difference between the measured velocities and the actual mean velocity of the channel increases but from w_r= 1 to w_r= 1.4 the cross section excessively increases in the branch channel and the discharges are constant therefore the velocities decrease and are less affected by the flow hydraulic in the separation zone and compression zone this decreases the difference between the measured velocities and the actual mean velocity of the channel.

CONCLUSION

Hydraulic structures such as intakes are used in rivers and channels to control the flow and to deviate a part of the flow. The flow velocity is measured by flowmeters to calculate the discharge passing through these channels. In order to evaluate the effect of the flowmeter location in the intake on the velocity measurement accuracy, the location of the flowmeter was examined through the ANSYS-CFX software in

three specific states for different w_r width rations in this study. The measured velocities were compared with the actual mean velocity of the channels in each of the w_rs. The results indicated that the obtained results are closer to the actual mean velocity of the channel for all w_rs when the flowmeter measures the longitudinal velocities in three vertical columns which are located in equal transverse distances. The difference between the measured velocities and the actual velocity of the channel had an ascending trade for all flowmeter locations from w_r= 0.6 to w_r= 1 with regard to the fact that the separation zone and the compression zone develop in this range however this trend is a descending one from w_r= 1 to w_r= 1.4 since the discharge is constant from w_r= 1 to w_r= 1.4 and the separation zone and the compression zone lesser affect the v* longitudinal velocities which decreases the difference between the measured velocities and the actual mean velocity of the channel. Therefore the difference between the measured velocities and the actual mean velocity of the channel has its maximum value in w_r= 1 among all other w_r due to the development of the separation zone and the compression zone and it reaches 100% in some points however this different decreases in w_r= 0.8, 0.6 and reaches its minimum value which is an average of approximately %5 .

REFERENCES

1. Lakshmana, R.N.S., Sridharan. K., Baig, M.Y.A., (1968).” Experimental study of the division of flow in an open channel”. Australasian Conf. on Hydraul and Fluid Mech, Sydney, Australia, 139-142.
2. Taylor, E., (1944). “Flow characteristics at rectangular open channel junction, Journal of Hydraulic Engineering. 10(6):893-902.
3. Ramamurthy, A., Qu, J., Vo, D., (2007). “Numerical and experimental study of dividing open-channel flows”. Journal of Hydraulic Engineering, 133(10):1135-1144.
4. Neary, V.S., Odgaard, A., Sotiropoulos, F., (1999). “Three-dimensional numerical model of lateral-intake inflows”. Journal of Hydraulic Engineering, 125(2):126-140.
5. Barkdoll, B.D., Hagen, B.L., Odgaard, A.J., (1998). "Experimental comparison of dividing open-channel with duct flow in T-junction". Journal of Hydraulic Engineering, 124(1): 92-95.
6. Issa, R.I., Oliveira, P.J., (1994). "Numerical prediction of phase separation in two-phase flow through T-junction", Comp. and Fluids, 23(2):347-356.
7. Law, S.W., Reynolds, A.J., (1966). "Dividing flow in an open Channel", Journal of Hydraulic Div. Vol.92, No2, pp.4730-4736.
8. Mignot, E. et al., (2012). "Experiments and 3D simulations of flow structures in junctions and their influence on location of flowmeters". Water Science and Technology, 66(6): 1325-1332.
9. Hager, W. H., (1992). “Discussion of ‘Dividing flow in open channels’ by A. S. Ramamurthy, D. M. Tran, and L. B. Carballada.” J. Hydraul. Eng., 118_4_, 634–637.
10. Wilcox, D. C., (2000). "Turbulence modeling for CFD", 2nd Ed., DCW Industries, Inc.
11. Olsen, N.B.R.,(2006). "A three-dimensional Numerical Model for Simulation of Sediment Movements in Water Intakes with Moltiblock Option", Department of Hydraulic and Environmental Engineering, The Norwegian University of Science and Technology.
12. Hsu, C. C., Tang, C. J., Lee, W. J., and Shieh, M.-Y., (2000). “Subcritical 90° equal-width open-channel dividing flow”, J. Hydraul.Eng., 128_7_, 716–720.
13. Tanaka, K., (1957), “The improvement of the inlet of the Power Canal.” Transactions of the Seventh General Meeting of I.A.H.R., 1, 17.
14. Ferziger, J. H., Peric, M., (2002), "Computational method for fluid dynamics", 3rd Ed., Springer, New York.
15. Shettar, A.S., Murthy, K.K., (1996). "A numerical study of division of flow in open channels". Journal of Hydraulic Research, 34(5):651-675.
16. Neary, V.S., Sotiropoulos, F., (1996)." Numerical investigation of laminar flows through 90-degree diversions of rectangular cross-section". Computational and Fluids, 25(2):95-118.
17. Kasthuri, B., Pundarikanthan, N.V., (1987). "Discussion of 'separation zone at open channel junction". Journal of hydraulic Engineering, 113(4):543-544.
18. Neary, V.S., Odgaard, A.J., (1993). "Three-dimensional flow structure at open channel diversions". Journal of Hydraulic Engineering, 119(11):1224-1230.
19. Hager, W.H., (1987). Discussion of “Separation Zone at Open-Channel Junctions” by James L. Best and Ian Reid (November, 1984). Journal of Hydraulic Engineering, 113(4): 539-543.
20. Chen, H. B., Lian, G. S., (1992). “The numerical computation of turbulent flow in t-junction” J.Hydrodynamics, 3, 16-25, 50-58.
21. Ramamurthy, A. S., Tran, D. M., and Carballada, L. B., (1990). “Dividing flow in open channels.” J. Hydraul. Eng., 116(3), 449–455.